Defence Technology 40 (2024) 138–153

Contents lists available at ScienceDirect

Defence Technology

journal homepage: www.keaipublishing.com/en/journals/defence-technology

# Comparative impact behaviours of ultra high performance concrete columns reinforced with polypropylene vs steel fibres

Thong M. Pham [a], Harrison Hyde [b], Maw K. Kaung [c], Yan Zhuge [a], Duong T. Tran [d], Des Vlietstra [e], Tung M. Tran [f, *]

[a] UniSA, STEM, University of South Australia, Mawson Lakes, SA 5095, Australia
[b] BG□E Pty Ltd, Wellington Street, Perth, WA, 6000, Australia
[c] Austral Construction Pty Ltd, St Georges Terrace, Perth, WA, 6000, Australia
[d] Centre for Infrastructural Monitoring and Protection (CIMP), Curtin University, Kent St, Bentley, WA 6102, Australia
[e] Barchip Australia Pty Ltd, U 2 6 Qualtroughq Street, Woolloongabba, Queensland, 4102, Australia
[f] Sustainable Developments in Civil Engineering Research Group, Faculty of Civil Engineering, Ton Duc Thang University, Ho Chi Minh City, 72915, Viet Nam

ARTICLE INFO

*Article history:*
Received 18 December 2023
Received in revised form
11 February 2024
Accepted 22 April 2024
Available online 4 May 2024

*Keywords:*
Ultra high-performance concrete
Steel fibre
Polypropylene micro-fibre
Fibre volume fraction
Impact loading
Pendulum tests
Columns

ABSTRACT

Polypropylene (PP) fibres have primarily used to control shrinkage cracks or mitigate explosive spalling in concrete structures exposed to fire or subjected to impact/blast loads, with limited investigations on capacity improvement. This study unveils the possibility of using PP micro-fibres to improve the impact behaviour of fibre-reinforced ultra-high-performance concrete (FRUHPC) columns. Results show that the addition of fibres significantly improves the impact behaviour of FRUHPC columns by shifting the failure mechanism from brittle shear to favourable flexural failure. The addition of steel or PP fibres affected the impact responses differently. Steel fibres considerably increased the peak impact force (up to 18%) while PP micro-fibres slightly increased the peak (3%–4%). FRUHPC significantly reduced the maximum mid-height displacement by up to 30% (under 20° impact) and substantially improved the displacement recovery by up to 100% (under 20° impact). FRUHPC with steel fibres significantly improved the energy absorption while those with PP micro-fibres reduced the energy absorption, which is different from the effect of PP-macro fibre reported in the literature. The optimal fibre content for micro-PP fibres is 1% due to its minimal fibre usage and low peak and residual displacement. This study highlights the potential of FRUHPC as a promising material for impact-resistant structures by creating a more favourable flexural failure mechanism, enhancing ductility and toughness under impact loading, and advancing the understanding of the role of fibres in structural performance.



## 1. Introduction

Vehicle collisions with bridge piers are a significant cause of bridge failures in the United States, accounting for approximately 15% of all such incidents [1]. The devastating consequences of these collisions were exemplified by the collapse of Grant Avenue overpass in New York in 1994, which resulted in the loss of one life, injury to 23 people, and a fire that spread over a radius of 122 m. Other sources of impact loading of concrete columns include earthquakes, vessel collisions, rockfalls, and even terrorist attacks [2–4]. While these events are relatively rare, the incidence of column failure due to impact loading is increasing, with severe consequences in terms of both economic loss and human casualties [5,6]. Under such conditions, normal strength concrete (NSC) columns may experience brittle failure and low toughness, posing a significant risk to structural systems such as bridges, car parks, and low-rise buildings. To mitigate this risk, research, development, and design efforts must prioritise the impact resistance of columns in future engineering applications.

Concrete columns are an essential structural component of various infrastructure systems such as bridges, car parks, and low-rise buildings. However, their vulnerability to impact loading can lead to catastrophic consequences, resulting in economic loss and casualties. To improve the impact resistance of concrete columns,

* Corresponding author.
*E-mail address:* tranminhtung@tdtu.edu.vn (T.M. Tran).
Peer review under responsibility of China Ordnance Society

https://doi.org/10.1016/j.dt.2024.04.016

various methods have been explored, such as strengthening with fibre-reinforced polymer (FRP), using a sacrificial layer or protective structures, or advanced materials [7–10]. One such material that has recently gained considerable attention is ultra-high- performance concrete (UHPC), which possesses superior properties such as high compressive and tensile strengths, excellent toughness, and durability [11–15].

UHPC was initially introduced in the 1990s as reactive powder concrete (RPC) before being used to reduce the self-weight and improve the corrosion resistance of the deck of the Sherbrooke footbridge in 1997, which was the first full-scale engineering application of UHPC [2,16]. The initial success and unique material properties of UHPC motivate its application and further development, particularly over the last eight years. Xue et al. [16] found that the number of publications concerning UHPC increased from 33 in 2015 to 109 in 2019. The increasing popularity of UHPC is directly related to the excellent material properties and potential for engineering applications. In addition to improved ductility, durability, impact resistance and fatigue resistance, UHPC typically has compressive and tensile strengths over 150 MPa and 8 MPa respectively as per [16,17] or the compressive strength of greater than 120 MPa regarding America's Cement Manufacturers [18]. The development of suitable properties of UHPC often relies on trialling and optimisation of a mix design and the appropriate application of heat or pressure curing. Therefore, current research focuses on the development of design guides that provide explicit relationships between material, preparation and treatment variables directly influencing the properties of UHPC [16,19–21].

The optimisation of fibre content in UHPC is a key consideration in producing a suitable mix design, particularly for concrete members subject to impact loading. Should fibres not be included in UHPC, the very high compressive strength and homogenous nature of the material result in brittle failure, a detrimental characteristic of NSC, especially under impact loads [20,22]. When included in appropriate quantities, fibres provide a crack-bridging effect, preventing the growth and propagation of cracks, increasing tensile, compressive and flexural strength, improving ductility and enhancing toughness [2,12,23]. However, there are two major issues associated with the use of fibres, the first of which is the material cost. Should a steel fibre volume content of 2% be selected, the cost of steel fibres makes up 60%–80% of the total cost of UHPC [24]. The other issue is the balling of fibres in traditional rotary drum mixers at excessive steel fibre contents, resulting in the loss of workability and reduction in mechanical properties [17,20,25]. Hence, further research is required on the influence of fibre content on the structural behaviour of UHPC members, particularly under impact loading [16].

In addition to the fibre volume fraction, different types of fibre affect the material properties and structural responses differently. There are many types of fibres used for ultra-high performance concrete columns in the construction industry such as steel, nylon, polypropylene, polyethylene, carbon, and plastic fibres [17]. These fibres affect the material properties differently [16,17,19]. Among these fibres, steel and carbon fibres are most commonly used in UHPC due to their high tensile strength and modulus. Polypropylene (PP) macro-fibres are however more affordable while providing good mechanical properties [26,27]. Previous studies found that PP fibres can significantly mitigate explosive spalling in concrete structures exposed to fire [28–31]. While there have been numerous studies on the material properties of UHPC, such as its tensile strength, fracture toughness, and flexural strength, there are relatively fewer investigations on the structural behaviour of UHPC structural components. There is still a lack of research on the structural performance of UHPC, particularly when comparing UHPC with steel fibres versus UHPC with PP macro-fibres.

This is particularly relevant when comparing the performance of concrete reinforced with different types of fibres. Ngo et al. [32] compared the structural performance of steel fibre-reinforced concrete (SFRC) joint vs PP macro-fibre reinforced concrete (PFRC) joint under impact loading. They found that the first one exhibited better structural performance (less damage and higher load) but lower energy dissipation capability as compared to the latter one. Similarly, Tran et al. [33] found that the use of steel fibres was more effective than PP macro-fibre in delaying the crack opening in fibre-reinforced geopolymer concrete due to the high modulus of steel fibres but PP macro-fibres yielded better post-peak performance. The geopolymer beam reinforced with PP macro-fibres exhibited lower maximum and residual displacement than its counterpart reinforced with steel fibre under the same impact condition. There is limited study on PP micro-fibre reinforced concrete under impact loading [34], particularly for structural members. Therefore, further research is needed to evaluate the structural performance of UHPC reinforced with steel fibres and PP micro-fibres in order to fully understand their potential applications in construction and infrastructure.

As can be seen above, there is a dearth of research on the structural performance of UHPC structures reinforced with steel fibres compared to those reinforced with PP fibres. Particularly, there is no comparative study on the structural performance of UHPC columns reinforced with steel fibres vs micro-PP fibres under lateral impact loads. Therefore, this study aims to investigate the effect of fibre type (steel vs micro-PP) and volume fraction on the impact behaviour of UHPC columns by using pendulum impact tests.

## 2. Experimental program

In this study, one NSC and five UHPC mix designs with three fibre volume contents (0%, 1%, and 2%) and two fibre types (steel and micro-PP) were used to cast columns.

### 2.1. Materials and mix design

#### 2.1.1. Aggregates and silica sand

For NSC, fine sand was used as fine aggregate whereas coarse aggregates were divided into two groups based on particle size. The maximum particle size of each group was 10 mm and 7 mm. This was consistent with a study by Pournasiri et al. [13] to ensure that suitable NSC properties are expected. The fine and coarse aggregates used in this project were supplied by Holcim (Australia) Pty Ltd. Although no coarse aggregate was used in UHPC, silica sand with a median particle size of 300 μm was used as the fine aggregate. The physical properties of silica sand can be found in Ref. [13].

#### 2.1.2. Portland cement and supplementary cementitious materials

Ordinary Portland cement complying with the requirements of AS 3972 [35] was used as the primary binding material in both NSC and UHPC. The Portland cement used in this project was supplied by Cockburn Cement. The supplementary cementitious materials (SCMs) including silica fume and fly ash were used in the mix design of UHPC. Silica fume and fly ash were supplied by SIMCOA Silica Fume [36] and Cement Australia. Fly ash class F with the chemical composition was presented in our previous study [37], which is not repeated herein for brevity.

#### 2.1.3. Superplasticiser and fibres

Superplasticiser was used in the preparation of all UHPC samples to achieve desirable workability. The third generation of high-range water reducer containing modified polycarboxilates, Sika ViscoCrete PC HRF-2, was selected and supplied by Sika Australia

Pty Ltd.

Dramix 3D bright glued steel fibres were included in each of the UHPC mix designs at volume proportions of 1% and 2%. The hooked-end steel fibres had a length of 35 mm and a nominal diameter of 0.55 mm (corresponding to the aspect ratio of 65). The nominal tensile strength and elastic modulus respectively were 1345 MPa and 210 GPa, as provided by the manufacturer [38].

The geometry and aspect ratio of fibres indeed play a crucial role in fibre-reinforced concretes. The aspect ratio, which is the fibre length divided by its diameter, and the volume fraction of fibres significantly influence the flexural strength of the concrete [39,40]. The fibre geometry, including the spatial distribution and orientation of the fibres, also affects the tensile strength of the specimens [41,42]. Fibres are normally divided into two main groups based on their size: macro-fibres and micro-fibres. Micro-fibres typically have diameters measured in tens of microns and 6–20 mm in length. Macro-fibres are typically 30–60 mm in length and have diameters exceeding 0.3 mm. Micro-fibres have gained widespread recognition for their effectiveness in controlling plastic shrinkage and arresting micro-cracks and shrinkage cracks [26,43]. Thus, the cracking strength of concrete can be significantly improved with micro-fibres. However, due to their short length, micro-fibres provide limited structural contribution when the structure is subjected to significant deformations. Macro-fibres possess the ability to bridge macro-cracks, bear loads and halt the development of visible cracks once the concrete matrix fractures, similar to reinforcement, thereby post-cracking behaviour and toughness of concrete can be improved with the use of using macro-fibres [26,44]. Steel fibres were used in this study based on outstanding mechanical characteristics and acknowledged efficacy in enhancing concrete structure's performance [45,46]. Polypropylene fibres were chosen for their environmentally friendly nature, resistance to chemicals, light weight, structural efficacy, and as an optimal solution to combat corrosion issues from steel.

Polypropylene (PP) micro-fibres, consisting of 100% polyolefin polymer, were used in the UHPC mix at volume proportions of 1% and 2%. The PP micro-fibres had a length of 12 mm and specific gravity of 0.91. The equivalent thickness was 32 mm and the melting point was 162 °C. The tensile strength and elastic modulus respectively were 650 MPa and 12 GPa, as provided by the manufacturer.

#### 2.1.4. Reinforcement

There were 3 different types of reinforcement used in the experiment, i.e., 6 mm steel reinforcement bars, 6 mm steel reinforcement mesh, and 4 mm steel wire for stirrups. ReoMart R6 processed 6 mm diameter steel reinforcing round bars were used as longitudinal reinforcement with a tensile strength of 250 MPa. Steel meshes were procured from ReoMart Pty Ltd. 4-mm steel bars were procured from Midalia Steel to produce the transverse reinforcement. The yield and ultimate strengths of 6 mm deformed bars were 555 MPa and 616 MPa, respectively. The corresponding values for 4 mm steel stirrups were 346 MPa and 430 MPa, respectively.

#### 2.1.5. Mix design

The mix design of NSC and UHPC was adopted from a previous study [13] and is presented in Tables 1 and 2. However, it was modified through a series of trial mixes and testing process, according to the available materials and equipment. The mixing process involves several sequential steps [47,48]. Initially, essential ingredients like cement, silica sand, and silica fume were poured into a 70 L mixer for a dry mixing duration of 5 min. Subsequently, 70% of the required water was gradually added, allowing for an additional 3 min of mixing. The superplasticizer, along with the remaining water, was then added to the cementitious mixture. The design mix underwent continuous mixing for approximately 10 min until achieving optimal workability and flowability. Finally, steel or PP fibres, depending on the specified volume fractions, are introduced into the mixer according to the requirements.

For ease of reference, each mix design was assigned an abbreviated name, e.g., "NSC" and "UHPC" respectively refer to normal strength concrete and ultra-high-performance concrete, "0%", "1%" and "2%" refer to the fibre content by volume in the concrete mixture, and "PP" and "SF" represent polypropylene and steel fibres, respectively.

### 2.2. Column design

The columns were designed to have a lumped mass on the column top, representing the mass of the superstructure of bridge piers, based on previous studies by Pham et al. [49] and Schoettler et al. [50] and in accordance with AS 5100.2:2017 [51]. The original column has dimensions of 1.22 m in diameter and 7.32 m in height as adopted in a previous study [52]. To accommodate the capacity of the pendulum testing system, a geometric scale factor of 1/12 was applied. The scaled column had a cylindrical shape with a height of 600 mm and a diameter of 100 mm. The bottom of the column was connected directly to a square footing with dimensions of 400 mm × 400 mm × 150 mm. For the sake of brevity, the scaled specimens are referred as columns in this study. Four holes were included at each corner of the footing to allow for the column to be secured to the strong laboratory floor by bolts, creating a rigid connection. The top of the column was connected directly to a column cap with dimensions of 500 mm × 500 mm × 150 mm. A small hole was provided to each corner of the cap to allow for mass blocks to be bolted to the column. The mass blocks provided inertial resistance to the column top under impact loading.

Longitudinal reinforcement consisted of four 6 mm diameter plain round bars, each of which was evenly spaced and extended 130 mm into the footing and cap. These bars were provided with a 90° bend at each end, extending a further 200 mm towards the corners of the footing and cap and providing the required anchorage. Transverse reinforcement was spiral stirrups around the outside of the longitudinal reinforcement. Each stirrup was produced from a 4 mm diameter steel bar deformed to provide a pitch of 50 mm and a radius of 80 mm. Finally, top and bottom reinforcement for the cap and footing was produced from 6 mm diameter square rib mesh with a spacing of 100 mm as shown in Fig. 1.

The required cover for UHPC is typically lower than NSC as an improved tensile capacity prevents steel exposure through concrete cracking and spalling [20]. However, as mentioned above, the reinforcement design was required to be consistent with the reference NSC column, so a cover of 20 mm was adopted for the footing and top slab while the concrete cover of the columns was 10 mm.

**Table 1**
NSC mix design ($kg \cdot m^{-3}$).

| Mix | Portland cement | Water | Coarse aggregate (≤10 mm) | Coarse aggregate (≤7 mm) | Sand |
|---|---|---|---|---|---|
| NSC | 426 | 205 | 444 | 436 | 843 |

**Table 2**
UHPC mix design ($kg \cdot m^{-3}$).

| Mix | Portland cement | Silica fume | Fly ash | Silica sand | Water | Superplasticiser | Steel fibre | PP micro-fibre |
|---|---|---|---|---|---|---|---|---|
| UHPC-0% | 800 | 154 | 77 | 1039 | 180 | 67 | – | – |
| UHPC-1%SF | 800 | 154 | 77 | 1039 | 180 | 67 | 78 | – |
| UHPC-2%SF | 800 | 154 | 77 | 1039 | 180 | 67 | 156 | – |
| UHPC-1%PP | 800 | 154 | 77 | 1039 | 180 | 67 | – | 9.7 |
| UHPC-2%PP | 800 | 154 | 77 | 1039 | 180 | 67 | – | 19.4 |

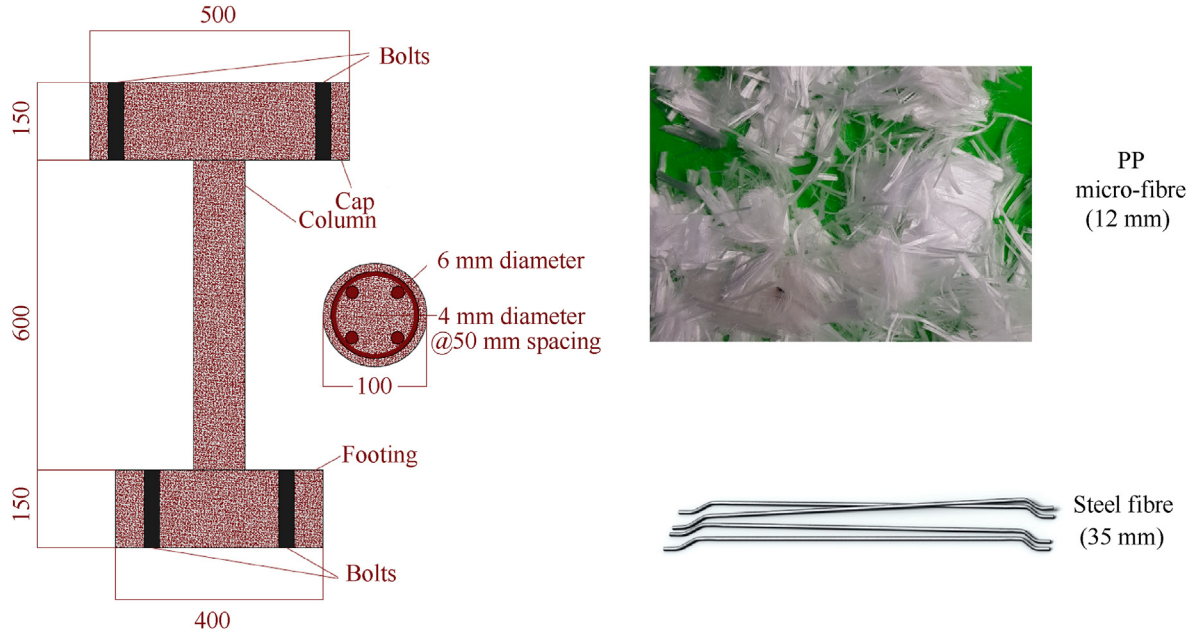


**Fig. 1.** Column dimensions and reinforcement (all dimensions in millimetre).

### 2.3. Casting and curing

The mixing and curing of NSC mix were based on AS 1012.2 [53]. Compaction of NSC cylinder samples was done on a vibrating table whereas a concrete vibrating poker was used for the columns. There were no standards available for the preparation of UHPC. Instead, mixing was based on the procedure used by previous studies [2,13,14]. For health and safety concerns, nanoparticles were not used but they are replaced by fine silica sand as also adopted by Refs. [13,14].

The curing method used for all columns and samples was based on an experimental study conducted by Refs. [13,14]. After an initial 24 h of ambient curing, samples were placed in a steam room, allowing for steam curing at the desired temperature of 85 °C and relative humidity of 95%. Following 48 h of steam curing, the UHPC samples were returned to ambient conditions until the day of testing.

### 2.4. Preliminary test results

#### 2.4.1. Slump test

The relatively low water-to-binder ratio of UHPC results in a significant reduction in workability without the addition of superplasticiser [17]. Previous studies have also revealed that an increase in steel fibre content further reduces the workability of a concrete mix due to balling of fibres and poor dispersion throughout the concrete matrix [20]. To ensure that each design mix achieved sufficient workability for pouring and compaction, a slump test was performed, using a mini-slump cone with a height of 116 mm and an upper and lower diameter of 38 mm and 76 mm, respectively. The results of the slump testing as per AS 1012.3.1 [54] are provided in Table 3.

#### 2.4.2. Compression test and indirect tensile test

To determine the compressive strength of each mix design, three identical cylinders of 100 mm × 200 mm were tested as per AS 1012.9 [55] and the results are tabulated in Table 4.

All three UHPC mix designs achieved an average compression strength of approximately 120 MPa, a significant increase from NSC. UHPC-0% experienced severe brittle failure whereas other fibre-reinforced UHPC showed a much more ductile failure mode.

An indirect tensile test was performed on three identical cylinders (150 mm × 300 mm) of each design mixture as per AS 1012.10 [56] and the results are provided in Table 4. A significant improvement in the tensile strength is observed for UHPC, particularly for the mixes with fibre reinforcement. Compared to UHPC-0%, UHPC-1%SF exhibited a remarkable 70% increase in the tensile strength, while further increasing the steel fibre content to UHPC-2%SF only resulted in a 23% increase. This suggests that the greatest benefits to tensile strength are achieved at lower steel fibre contents. On the other hand, adding PP micro-fibres to the UHPC mix slightly reduced the compressive strength by 10% but considerably improved the split tensile strength by 18% as shown in Table 4.

### 2.5. Pendulum impact test

All the columns were tested under a pendulum impact rig as shown in Fig. 2. The columns were fixed at the footing and free at

**Table 3**
Slump test results.

| Mix Design | NSC | UHPC-0% | UHPC-1%SF | UHPC-2%SF | UHPC-1%PP | UHPC-2%PP |
|---|---|---|---|---|---|---|
| Slump/(mm × mm) | 90 × 80 | 195 × 190 | 170 × 155 | 125 × 120 | 92 × 103 | 80 × 100 |

**Table 4**
Results of compression tests.

| Mix Design | Compressive strength/MPa | Standard deviation | Split tensile strength/MPa | Standard deviation |
|---|---|---|---|---|
| NSC | 36.61 | 2.45 | 2.47 | 0.13 |
| UHPC-0%* | 117.68 | 3.70 | 7.51 | 0.33 |
| UHPC-1%SF | 122.05 | 3.28 | 12.80 | 1.46 |
| UHPC-2%SF | 120.86 | 3.50 | 15.70 | 2.19 |
| UHPC-1%PP | 106.48 | 5.34 | 9.05 | 1.42 |
| UHPC-2%PP | 106.48 | 3.64 | 8.73 | 1.04 |

Note: *Modulus of elasticity was approximately 41 GPa.

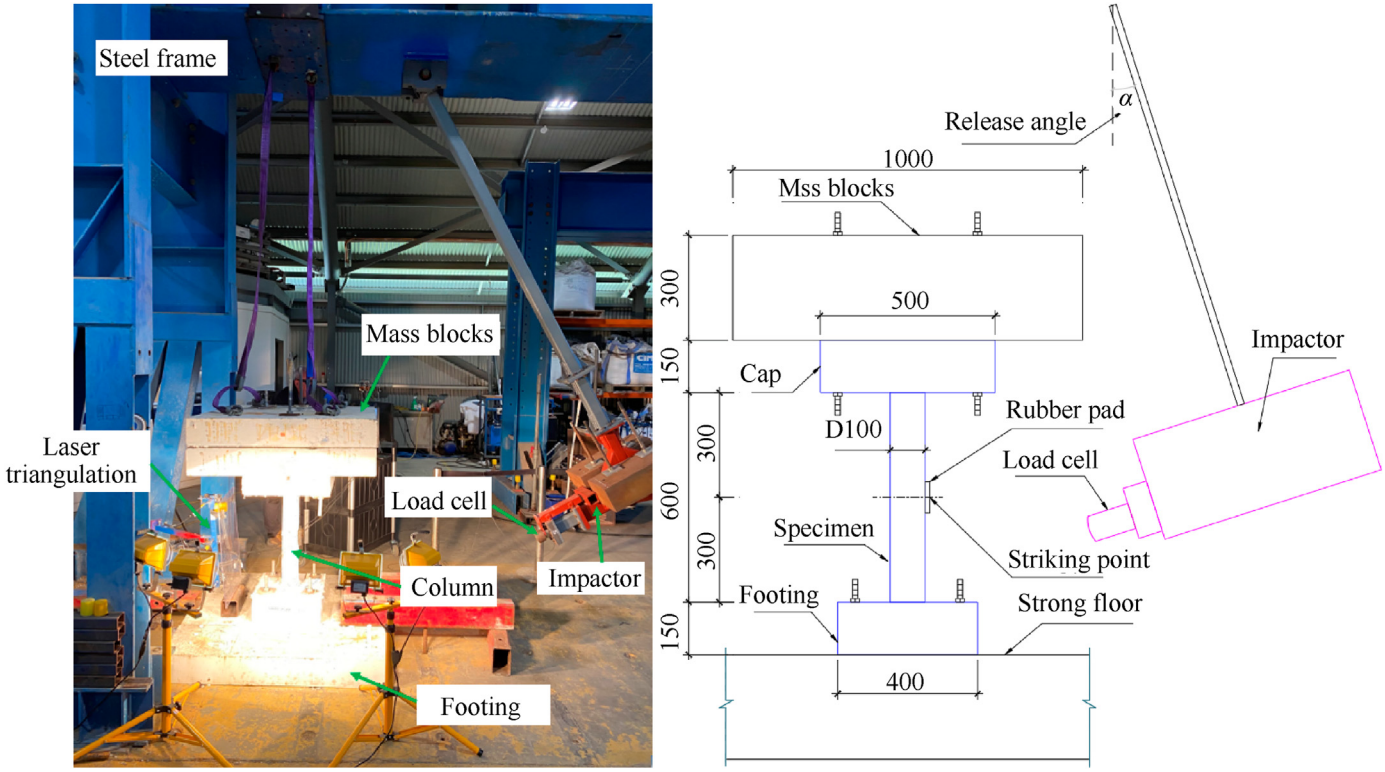


**Fig. 2.** Pendulum impact test.

the column cap. The footing was anchored to a concrete base, which was fixed to the strong floor, by using four 20-mm bolts. Two concrete blocks were fixed to the column cap to represent the weight and inertia resistance of superstructures. The two concrete blocks were measured 1000 mm × 1000 mm square and 150 mm thickness. The weight of each concrete block was 375 kg, making the total added mass on the column top 750 kg.

The pendulum arm was made of square hollow section steel (75 mm × 75 mm × 6 mm) and bolted to a hinge connection welded to the steel rigid frame. The pendulum arm had a total mass of 93 kg and extended 2.54 m from the hinge support. Two solid steel block weighing 300 kg was attached to the pendulum arm, making the total weight of the impactor 393 kg. After an initial impact test at a release angle of 5°, further tests were performed at release angles of 20° and 30°, which are equivalent to the impact velocity of 0.44 m/s, 1.73 m/s, and 2.58 m/s, respectively. The columns were struck at mid-height. The impactor hits the column and bounces back, deliberately pulled away to prevent a second impact on the column.

The impact response and progressive damage of the columns were monitored by using a high-speed camera with a sampling rate of 20,000 frames per second. Tracking points along the columns and impactor were used to trace the displacement of the column and the actual impact velocity of the impactor by using the image processing technique. The impact force was measured by using a 500-kN load cell attached to the impactor head. The impactor head was made from a steel cylinder with a diameter of 50 mm and the radius of the impactor nose was 250 mm. A laser triangulation was used to monitor the deflection of the impact point of the columns. The load cell and laser triangulation were connected to a data logger with a sampling rate of 96,000 Hz. No filter was used for the impact force acquisition.

A square natural rubber pad measuring 90 mm × 90 mm × 13 mm was used as an impact interlayer to create a soft impact condition [57,58]. The contact condition significantly affects the impact response of structures, which has been documented in previous studies [59,60]. The actual contact condition, in reality, varies, e.g., the bumper of a vehicle softens the contact stiffness in a vehicle collision event, soft layer on some guardrails and protective structures reduce the contact stiffness. The hard contact condition, i.e., steel impactor and concrete, was commonly adopted in many previous studies [59–67], probably because it is straightforward to be implemented in the impact tests. In this study, the soft contact condition is adopted in the tests. The rubber pads were sourced from Granor Rubber & Engineering, Australia with a hardness of 60 IRHD Duro±5. The rubber pad was replaced after every single impact to ensure a consistent impact condition.

## 3. Results and discussion

Each column was subjected to a series of lateral impact loads at its mid-height with increasing impact velocity. After an initial test at a release angle of 5°, further tests were conducted at 20° and 30°, corresponding to the designed impact velocities of 0.44 m/s, 1.73 m/s, and 2.58 m/s, respectively. However, the actual impact velocities of each impact were traced from the footage obtained from the high-speed camera by using an image processing technique. The high-speed camera was also used to monitor the impact response and failure mechanism of each column during and immediately after impact loading. The impact force-time histories were recorded using a load cell attached to the pendulum impactor. Deflection-time histories were recorded for the mid-height of each column using laser triangulation.

### 3.1. Failure mechanism

#### 3.1.1. General response and progressive failure

Responses of RC columns under lateral impact force were generalised by Pham et al. [68] who classified the column responses into two different phases, i.e., local response and global response. The local response is primarily governed by the shear behaviour of the localised region of the column vicinity to the loading point upon impact. After the stress waves propagate backward and forward a few times, the global responses become dominant. Accordingly, a cantilever column experiences flexural cracks at both sides (see Fig. 3) which are different from those under static loads where only one side experienced damage. Although the column size, section shape and contact conditions in this study are different from the previous study by Pham et al. [68], the observed results confirm this generalised response of RC columns under lateral impact loads.

The initial impact at a release angle of 5° (0.44 m/s) was used to study the elastic impact response of the columns. In all the columns, the low impact velocity induced mostly elastic vibration and no visible cracks were observed. The following analyses are focused on the impacts of 20° and 30°.

When the release angle was increased to 20° (1.73 m/s), flexural cracks directly behind the impact point and along the column and diagonal shear cracks formed. Minor spalling at the ends of Columns NSC and UHPC-0% were also observed. The third test at a release angle of 30° (2.58 m/s) resulted in the growth of existing cracks, major spalling damage and visible plastic deformation. Under this impact velocity, differences in the impact response and failure mechanism of these columns became evident. A comparison of the impact response and progressive failure of each column from a release angle of 30° is provided in Fig. 4 below.

All the columns failed by the combination of local and global modes under 30° impact (2.58 m/s). The progressive failure of all the columns shown in Fig. 4 above clearly resembles the local and global response phases described by Ref. [68]. During the local response phase, the initial impact of the pendulum resulted in the growth of existing cracks at the impact point. In Column NSC, UHPC-0%, UHPC-1%SF and UHPC-1%SF, diagonal shear cracks were formed and widened whereas the pre-existing flexural crack behind the impact face of Columns UHPC-2%SF and UHPC-2%PP continued to grow. The growth of both shear and flexural cracks was observed in UHPC-1%SF and UHPC-1%PP.

#### 3.1.2. Effect of fibre content and fibre type

During the global response phase, the deformation of the column became noticeable, and cracks located around the column cap and footing began to grow. During this period, shear cracks and major spalling appeared at the impact point of Column NSC and along the entire impact face above the mid-height of Column UHPC-0% (see Fig. 4). Closer inspection also revealed that the transverse reinforcement of Column UHPC-0% was exposed. The spalling concrete and brittle shear failure caused severe damage to

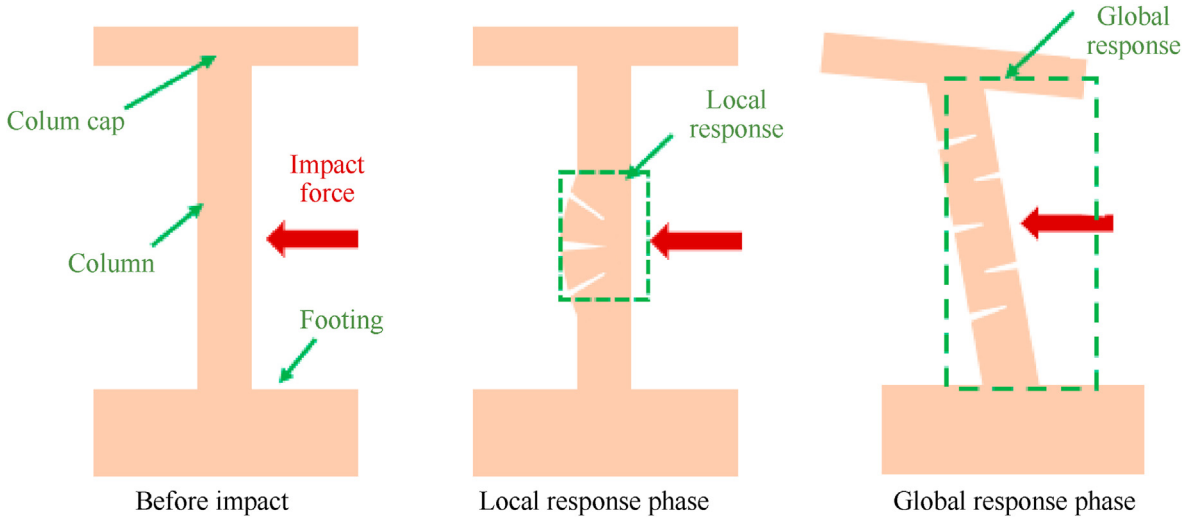


**Fig. 3.** Generalised response of RC columns under lateral impact (adopted and revised from Ref. [68]).

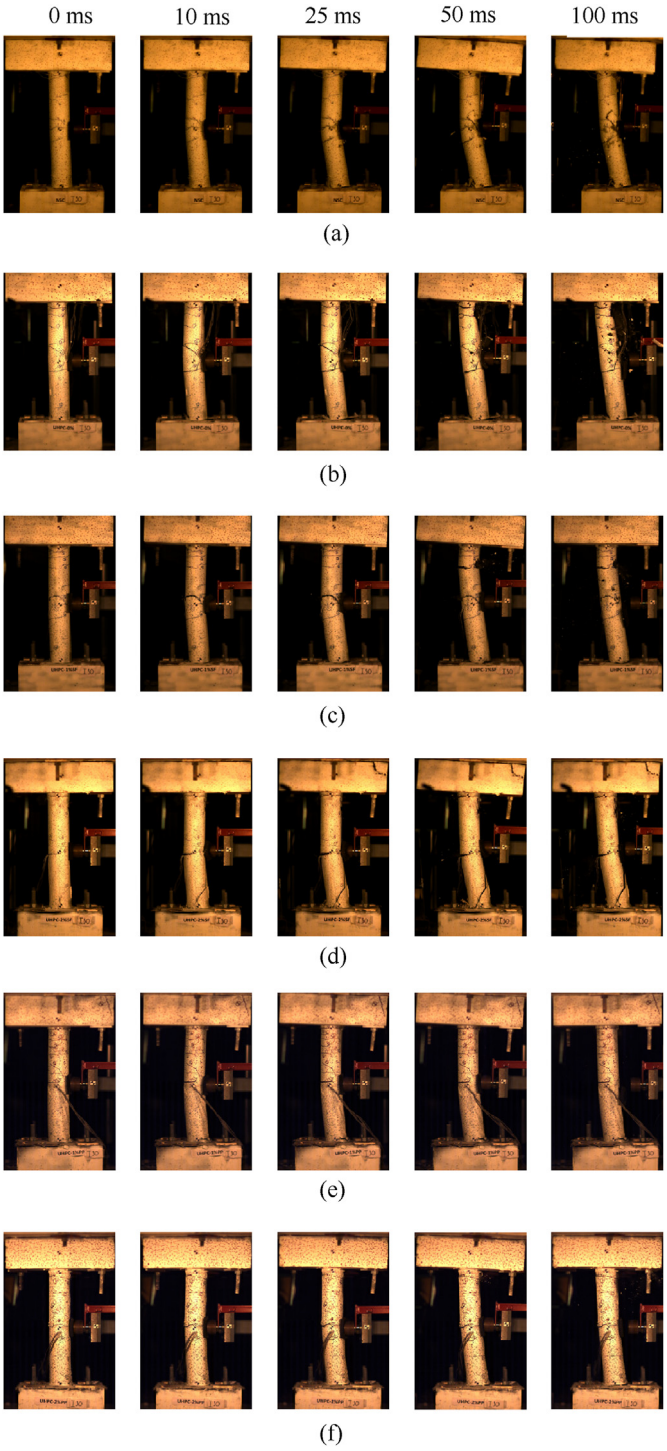


**Fig. 4.** Progressive failure under 30° impact (2.58 m/s): (a) NSC; (b) UHPC-0%; (c) UHPC-1%SF; (d) UHPC-2%SF; (e) UHPC-1%PP; (f) UHPC-2%PP.

Column UHPC-0%. Compared to Column NSC, Column UHPC-0% exhibited more severe shear and flexure cracks and concrete spalling due to higher impact force and the very brittle nature of unreinforced UHPC as shown in Fig. 5. Therefore, despite an improved compressive strength, the application of UHPC without fibres is not advisable for columns at risk of impact loading without measures to improve tensile and flexural strength, crack control and ductility.

For the fibre-reinforced UHPC columns, the tensile strength and thus the shear resistance was significantly improved. The shear behaviour became less prominent and even diminished in the UHPC columns with high fibre dosage. For example, Column UHPC-1%SF had less flexural cracks and only one inclined crack was observed at the impact point while Column UHPC-2%SF only experience one major cracks at the mid-height together with minor cracks, indicating significantly improved performance. It is worth noting that there was a major shear crack at the base of Column UHPC-2%SF due to a casting defect. Because the slump of UHPC-2% SF was significantly reduced, concrete was not completely filled in the corner of the formwork. A new layer of UHPC was added to this hole before curing in the steam room. Therefore, the shear failure at the base of Column UHPC-2%SF was due to imperfection of casting. It is noted that this casting difficulty was also reported in previous studies [17,20], which found that the inclusion of excessive fibres in UHPC may produce insufficient workability to achieve a fully homogeneous concrete mix.

Similarly, the use of PP micro-fibre also affected the impact behaviour and changed the failure mode. Compared to Columns NSC and UHPC-0%, Column UHPC-1%PP experienced less severe shear damage with only one shear crack near the impact point. The response of Column UHPC-2%PP was much different at which only one major flexural crack at the impact point was found with no shear crack. The number of cracks of the UHPC columns reinforced with PP was less than that of the UHPC columns reinforced with SF. In general, the use of fibre-reinforced UHPC significantly reduced the number of cracks and crack width and FRUHPC also changed the failure mode from the mix mode of shear-flexure to pure flexure as shown in Fig. 6.

The existing shear crack in Column UHPC-0% grew under the 30° impact but it was less severe than Column NSC. The failure surface of the columns also changed, evidenced by a smaller angle of the shear crack against the horizontal axis in Column UHPC-0%SF as compared to that of Column NSC. Column UHPC-2%SF showed no visible shear crack but the crack width of its major flexural crack was larger than the other two columns. For the influence of fibre type, the application of PP micro-fibre also yielded similar outcomes. Only one diagonal shear crack with a smaller angle was observed in Column UHPC-1PP while Column UHPC-2%PP exhibited no shear crack with a major flexural crack at mid-height. The above observations demonstrate that an increase in fibre content affected the failure mechanism of a UHPC column from brittle shear to flexural failure which does not result in a sudden loss of bearing capacity, providing forewarning of structural damage and preventing the disproportionate collapse of a structure.

### 3.2. Impact force time history

Impact force-time histories of all the columns are presented in Fig. 7. The impact force time history has a mountain shape before and after the peak impact force, where the impact force quickly increases to the peak and plummet to a low value before slowly diminishing. Due to a timing error, the impact force-time history was not acquired for the impact with the NSC column under 30° impact. A summary of the impact force time histories is provided in Table 5. Under 5° impact, the peak impact force of these columns was about 10–15 kN and it did not experience any noticeable difference in both the peak impact force and impact duration. The impact force increased gradually to its peak at about 20 ms and diminished at about 45 ms.

On the other hand, the impact force time histories of the columns under 20° and 30° impact increased steeply to their peak at about 10 ms, which was much faster than the case of 5° impact. The peak impact force of Column UHPC-0% under 20° impact was

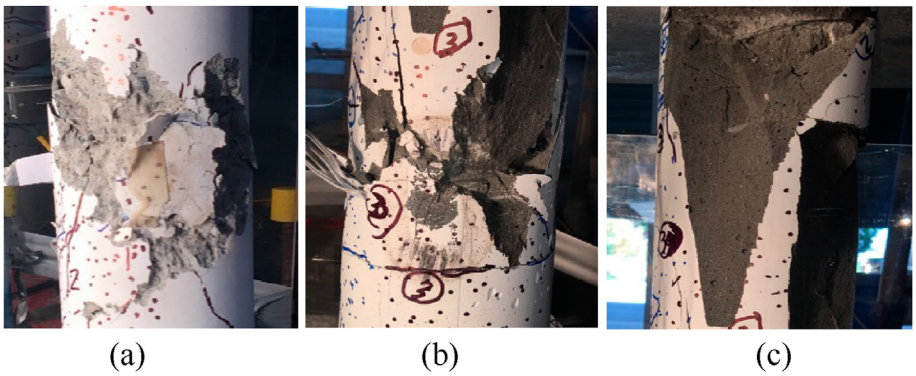


**Fig. 5.** Local spalling damage: (a) NSC mid-height; (b) UHPC-0% mid-height; (c) UHPC-0% top.

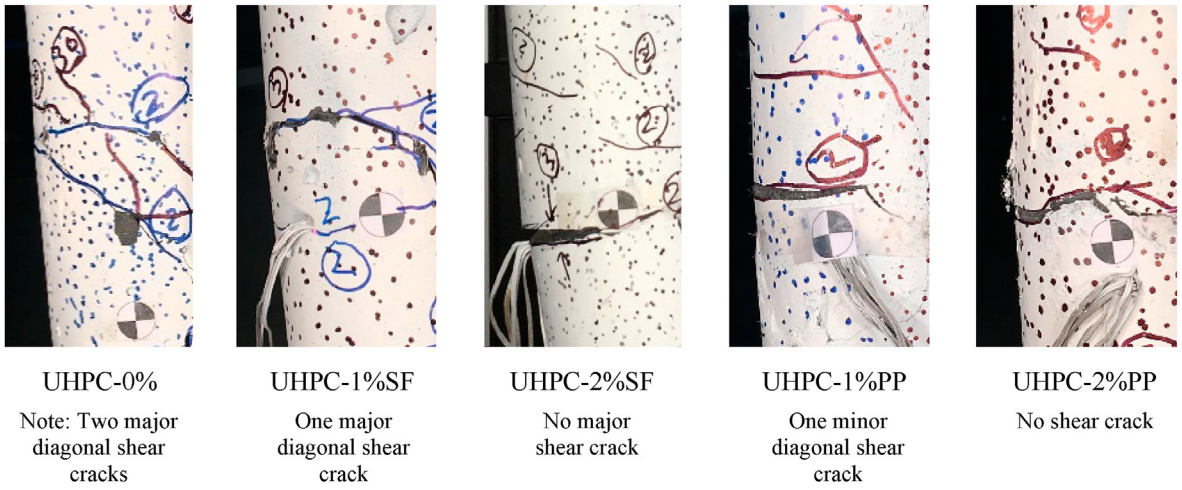


**Fig. 6.** Concrete damage at mid-height after 30° impact.

significantly higher than that of Column NSC (69 kN vs 55 kN). Compared to Column UHPC-0%, Columns UHPC-1%PP and UHPC-2%PP only exhibited a minor increased (3%–4%) in their peak impact forces of 71 kN and 72 kN under 20° impact, respectively, while the corresponding peak impact force of Columns UHPC-1%SF and UHPC-2%SF were respectively 82 kN and 78 kN, showing an increase of 13%–18%. These observations can be explained based on the column's stiffness. Previous studies have proven that the local stiffness primarily affects the first peak impact force while the global stiffness governs the global beam's response after the peak [64,65,69,70]. The local stiffness is governed by the contact stiffness and local shear stiffness. The shear stiffness is associated with the shear strength of concrete whereas the contact stiffness of the columns is governed by the elastic modulus of concrete and contact area. While the contact area can be assumed constant for these columns, the modulus of concrete was higher for UHPC reinforced with steel fibres. The higher the shear strength of concrete, the higher the local shear resistance and stiffness of the column. Similarly, the higher modulus of elasticity of concrete, the greater the contact stiffness.

From Table 3, both the compressive and tensile strengths of UHPC-0% were significantly higher than those of NSC. The local contact and shear stiffness of Column UHPC-0% were substantially greater than those of Column NSC, leading to substantial higher peak impact force of the first one as also observed. Besides, Columns UHPC reinforced with PP micro-fibres had a ~9.6% lower compressive strength and 20% higher tensile strength as compared to those of UHPC-0%. Collectively, the local stiffness and resistance of Columns UHPC-1%PP and UHPC-2%PP were inferred to be slightly higher than that of Column UHPC-0%. As expected, the peak impact force of Columns UHPC-1%PP and UHPC-2%PP under 20° impact was higher than that of Column UHPC-0% by 3%–4%. On the other hand, both the compressive and tensile strength of Columns UHPC reinforced with steel fibres were ~3% and 90% higher than those of UHPC-0%. As a result, the local stiffness and resistance of UHPC with steel fibres was expected considerably greater than that of UHPC-0%, which agreed with an increase of 13%–18% in their peak impact force under 20° impact regarding Column UHPC-0% (see Fig. 8).

In general, under 20° impact, the peak impact force of Column UHPC-0% was considerably greater than that of Column NSC while fibres have a different influence on the impact force of the UHPC columns. The use of PP micro-fibre only marginally increased the peak impact force of UHPC while the use of steel fibre can noticeably grew the peak impact force. This observation is attributed to the effect of fibres on the local stiffness of the columns as discussed above, and it might be valid only when no pre-damage from a previous impact was observed. After the 20° impact, these columns experienced different damage severity levels. Columns UHPC-1%PP and UHPC-2%PP exhibited less damage as compared to Columns UHPC-1%SF and UHPC-2%SF. Therefore, the local stiffness of Columns UHPC-1%PP and UHPC-2%PP might be greater than that of UHPC-1%SF and UHPC-2%SF even though the mechanical properties of the later ones were higher. As evident, the peak impact force of

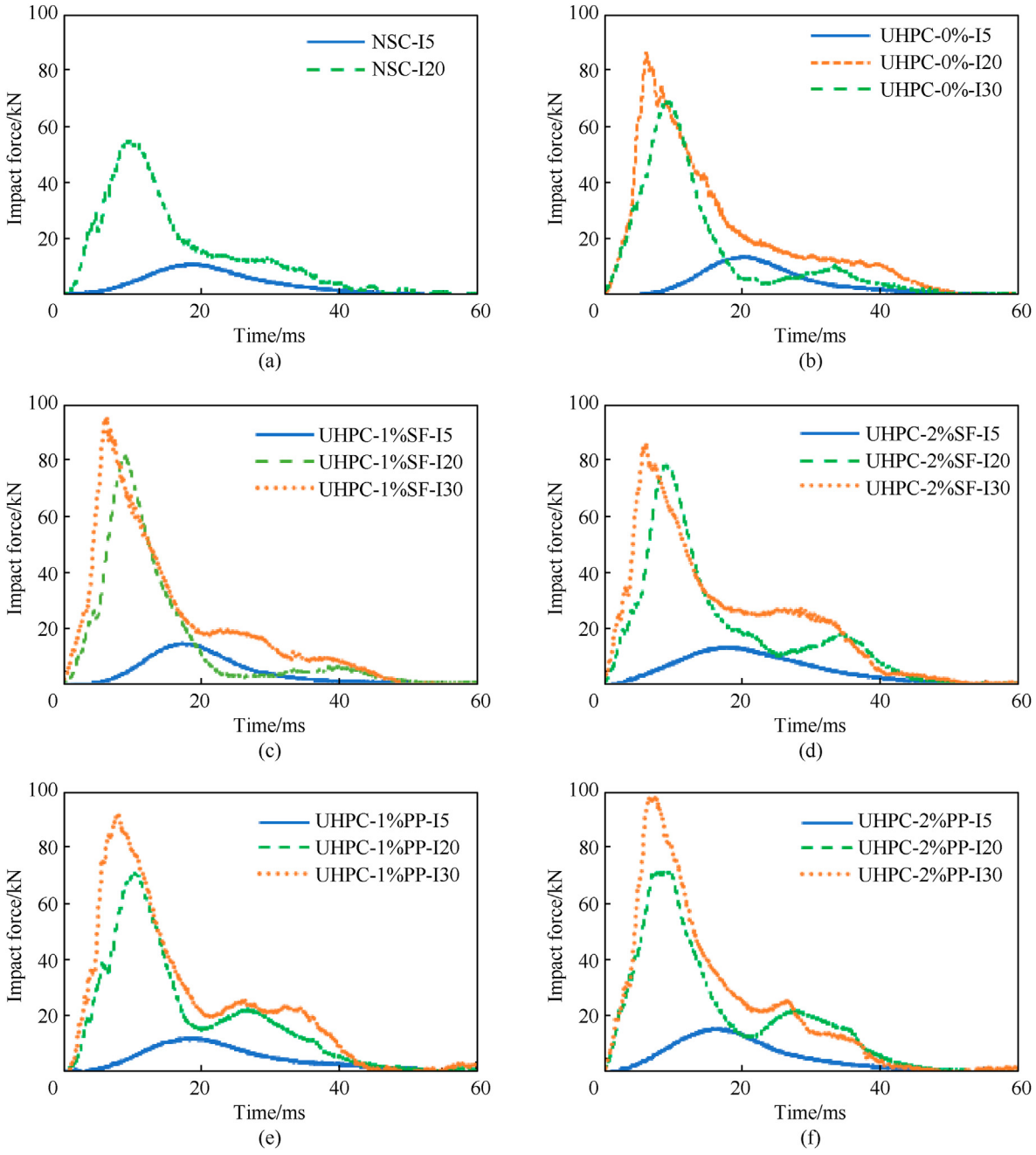


**Fig. 7.** Impact force-time histories of all the tested columns: (a) NSC; (b) UHPC-0%; (c) UHPC-1%SF; (d) UHPC-2%SF; (e) UHPC-1%PP; (f) UHPC-2%PP. Note: I5, I20, and I30 represent the release angle of 5°, 20°, and 30°, respectively.

UHPC-1%PP and UHPC-2%PP was slightly greater than that of UHPC-1%SF and UHPC-2%SF under 30° impact (see Fig. 8).

While the use of different types of concrete affected the peak impact force, the impact duration of all the columns under all impacts was almost the same. This observation is interesting and can be explained based on the global stiffness. A previous study reported that the impact duration becomes longer for specimens with lower global stiffness [71]. The lower global stiffness results in less resistance to stop movement of the impactor. As a result, a longer duration is required to slow down the movement of the structures till zero and thus the impact duration. The impact duration is thus primarily governed by the global stiffness of columns in this slow-impact condition. When the global vibration mode of these columns was obtained, they vibrated as a cantilever with the free end on their top. The global stiffness ($EI$) of a cantilever column with a circular section can be estimated as $EI = \frac{\pi}{4} Er^4$ ($r$ is the effective radius of the section and $E$ is the modulus of concrete). Accordingly, the effect of the effective radius is greatly more important than the elastic modulus of concrete. Similarly, the experimental results from this study have shown that the impact duration of all the columns under all impact tests was quite consistent, i.e., ~45–50 ms.

In general, the peak impact force of the UHPC columns was greater than that of NSC due to the higher modulus of concrete and local stiffness. The addition of fibre in UHPC only slightly changed the local stiffness of the columns and its effect was based on the

**Table 5**
Summary of impact force-time histories.

| Column | Impact velocity/(m·s$^{-1}$) | Peak impact force/kN | Impulse/(kN·ms) |
|---|---|---|---|
| NSC | 0.44 (5°) | 11 | 219 |
| | 1.73 (20°) | 55 | 827 |
| UHPC-0% | 0.44 (5°) | 14 | 252 |
| | 1.73 (20°) | 69 | 820 |
| | 2.58 (30°) | 87 | 1196 |
| UHPC-1%SF | 0.44 (5°) | 15 | 259 |
| | 1.73 (20°) | 82 | 884 |
| | 2.58 (30°) | 95 | 1239 |
| UHPC-2%SF | 0.44 (5°) | 14 | 292 |
| | 1.73 (20°) | 78 | 1076 |
| | 2.58 (30°) | 86 | 1416 |
| UHPC-1%PP | 0.44 (5°) | 12 | 253 |
| | 1.73 (20°) | 71 | 1057 |
| | 2.58 (30°) | 92 | 1481 |
| UHPC-2%PP | 0.44 (5°) | 16 | 288 |
| | 1.73 (20°) | 72 | 1103 |
| | 2.58 (30°) | 98 | 1399 |

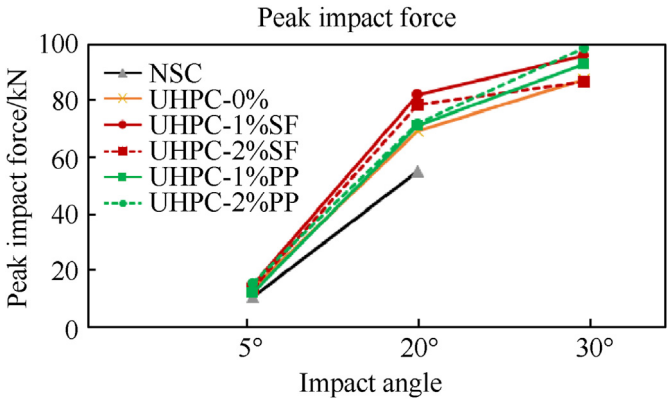


**Fig. 8.** Peak impact force of all the tested columns.

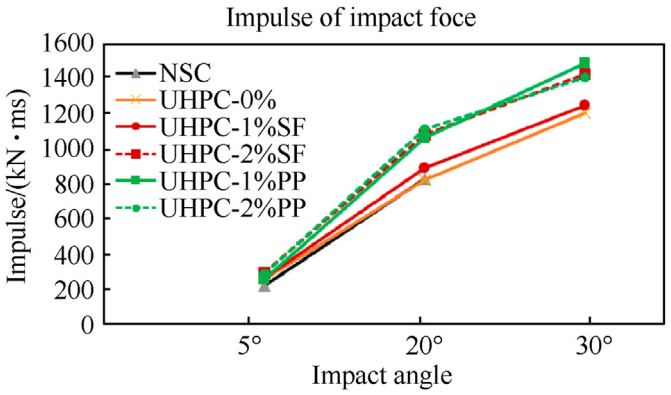


**Fig. 9.** Impulse of the impact force of all the tested columns.

type of fibres. As a result, the peak impact force of the UHPC columns reinforced with PP micro-fibres was only slightly higher than that of the reference UHPC column without fibre. The use of steel fibre increased the peak impact force more obviously regarding the reference UHPC column. However, if concrete columns were damaged due to the previous impact (i.e., 20° impact), the peak impact force of the following impact was significantly affected by the damage level.

To further quantify the impact performance of these columns, the impulse of the impact force of these columns was estimated as shown in Fig. 9. The use of PP micro-fibre showed a similar impulse as Column UHPC-2%SF and higher than that of Column UHPC-1%SF. It indicates that the excellent capability to dissipate impact energy of the UHPC columns with micro- PP fibre and the performance of Column UHPC-1%PP was similar to Column UHPC-2%PP. The use of 1% PP micro-fibre reinforcement is the optimum value in terms of fibre type and fibre content.

As suggested by Wei et al. [2], the inclusion of steel fibres at a volume content of 2% in UHPC accounts for 60%–80% of the total material cost. However, the financial investment associated with increasing steel fibre content did not considerably improve impact performance. When steel fibre content was increased from 1% to 2%, the impact from a release angle of 30° produced a major diagonal shear crack at the column base where only minor cracking had previously been identified. The major shear crack resulted from a plane of weakness in Column UHPC-2%SF due to the low workability of the concrete mix with high fibre content. Although improvements could be made to the design mix and preparation method, a high fibre content in UHPC is likely to create difficulty in mixing and casting samples, resulting in defects in structures [20,72]. The inclusion of steel fibres at a volume content of 2% will improve upon the failure mechanism of NSC and UHPC but will not necessarily improve the impact capacity unless further improvements to workability are made.

### 3.3. Deflection time history

Deflection-time histories, recorded using a laser triangulation positioned at column mid-height directly behind the impact face, are presented in Fig. 10. Due to a timing error, deflection-time history was not acquired for the impact with the NSC column from a release angle of 30°. It was unexpected but due to the very sophisticated nature of the test, this test could not be redon. In addition, this result does not considerably affect the discussion and conclusion in this study. Comparisons can be made on the displacement of other impacts and other measures can be also adopted to support the findings. A summary of key parameters derived from the displacement time histories is provided in Table 6. The mid-height displacement of these columns rapidly rose to the peak value upon impact. When the impactor was separated from the columns, the columns bounced back and entered a free-vibration phase and rested at their new stationary position, resulting in residual displacement.

In general, the shape of the mid-height deflection-time history

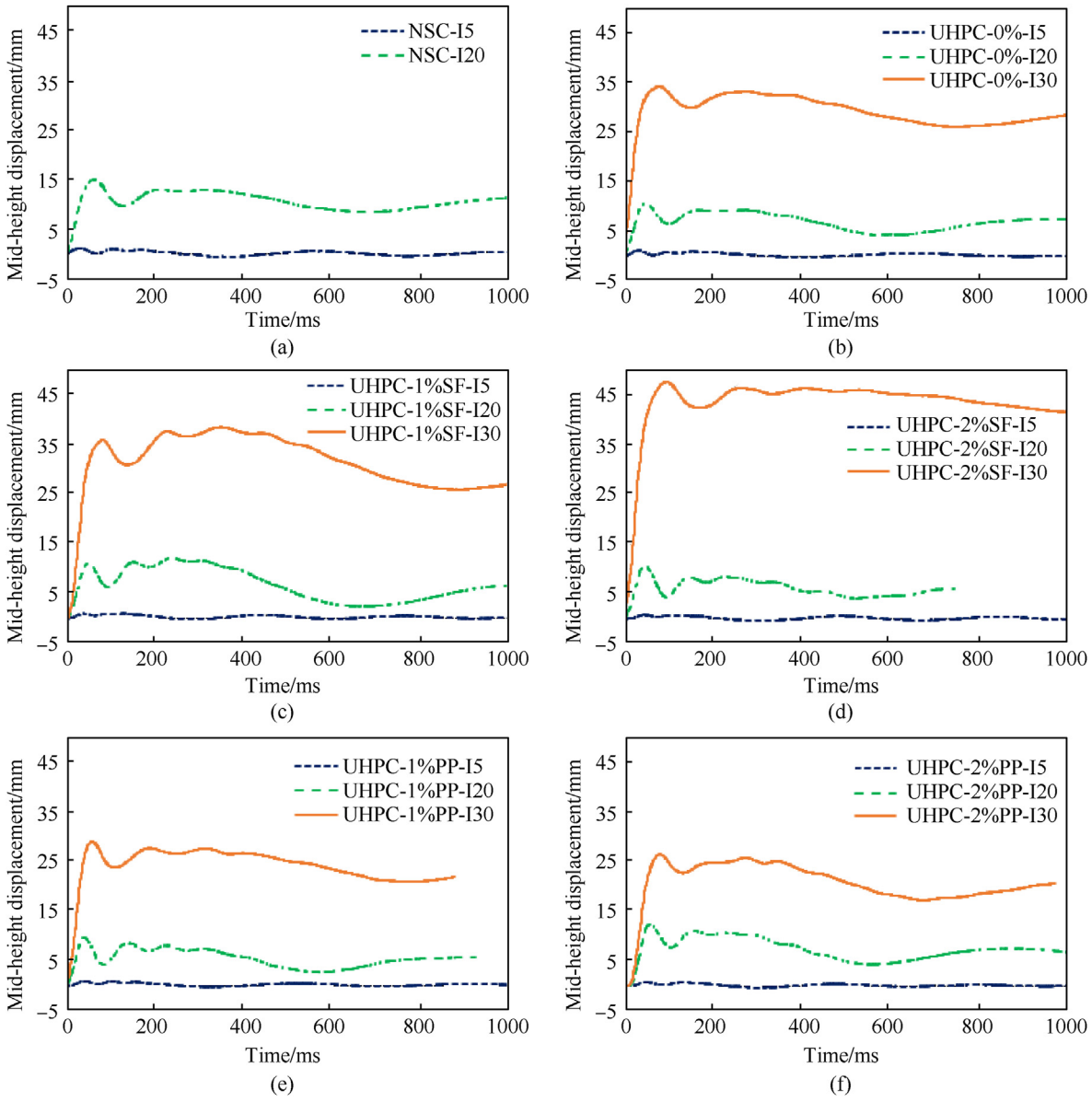


**Fig. 10.** Mid-height deflection-time histories of all the columns: (a) NSC; (b) UHPC-0%; (c) UHPC-1%SF; (d) UHPC-2%SF; (e) UHPC-1%PP; (f) UHPC-2%PP.

was similar for every impact test with an initial rapid rise in deflection before fluctuation about a slightly lower residual deflection. For each test at a release angle of 5° (0.44 m/s), the peak deflection did not exceed 1.3 mm with each column rebounding back to almost the same position after impact, indicating a complete elastic response. The elastic response of the columns to the first impact was expected and in agreement with all the impact force-time histories under the same loading conditions. As the release angle was increased to 20° (1.73 m/s), the peak deflection and residual deflection significantly increased. The percentage recovery of the peak deflection was significantly reduced (34%–62%) from the previous test due to plastic deformation. It is worth noting that the displacement recovery is the ratio of the elastic displacement (= peak displacement - residual displacement) and the peak displacement. This trend continued under the 30° impact tests where plastic deformation became obvious and the percentage recovery of peak deflection ranged between 15% and 28%, except UHPC-2%SF due to defect.

*3.3.1. Under 20° impact (1.73 m/s)*

The use of UHPC0% and FRUHPC significantly affected the maximum and residual displacement of the columns as shown in Fig. 11. The maximum and residual displacement of Column NSC was 14.7 mm and 10 mm, respectively. Column UHPC0% experienced a significant reduction of 25% for the maximum displacement and 35% for the residual displacement.

Column NSC had a residual mid-height displacement of 10 mm under 20° impact, corresponding to a 34% recovery from peak displacement. In contrast, the residual displacement of the UHPC columns fell between 4.3 and 6.4 mm, a significant reduction as compared to Column NSC. Column UHPC-0% slightly increased the mid-height displacement recovery to 40%. The use of fibre reinforcement significantly improved the mid-height displacement recovery up to 62% for Column UHPC-1%SF. As deflection recovery indicates the balance between elastic and plastic behaviour, the greater displacement recovery of UHPC columns demonstrates an improvement in capacity to absorb impact loads when compared to

**Table 6**
Experimental results of the column deflection.

| Columns | Impact Type | Top | | Mid-Height | | Bottom | | *Mid-Height Recovery/% |
|---|---|---|---|---|---|---|---|---|
| | | Peak Disp./mm | Residual Disp./mm | Peak Disp./mm | Residual Disp./mm | Peak Disp./mm | Residual Disp./mm | |
| NSC | 5° | 2.2 | 0.1 | 1.3 | 0.0 | 0.2 | 0.0 | 100 |
| | 20° | 20.8 | 14.0 | 15.1 | 10.0 | 2.3 | 1.5 | 34 |
| UHPC-0% | 5° | 2.5 | 0.7 | 1.3 | 0.2 | 0.2 | 0.0 | 84 |
| | 20° | 17.0 | 10.0 | 10.8 | 6.4 | 1.6 | 0.0 | 40 |
| | 30° | | 45.0 | 34.3 | 29.0 | | 3.7 | 15 |
| UHPC-1%SF | 5° | 2.0 | 0.4 | 1.0 | 0.1 | 0.3 | 0.1 | 90 |
| | 20° | 20.9 | 5.8 | 12.2 | 4.6 | 1.8 | 0.9 | 62 |
| | 30° | 57.2 | 36.0 | 38.5 | 29.0 | 4.8 | 3.6 | 25 |
| UHPC-2%SF | 5° | 1.5 | 0.1 | 0.8 | 0.1 | 0.2 | 0.0 | 88 |
| | 20° | 15.4 | 8.3 | 10.5 | 5.7 | 1.9 | 0.6 | 46 |
| | 30° | 66.7 | 59.0 | 47.6 | 43.0 | | 5.4 | 10 |
| UHPC-1%PP | 5° | 1.7 | 0.0 | 0.9 | 0.1 | 0.2 | 0.1 | 89 |
| | 20° | 15.8 | 5.9 | 9.7 | 4.3 | 2.2 | 1.3 | 56 |
| | 30° | 39.4 | 25.0 | 29.0 | 22.0 | 5.6 | 3.0 | 24 |
| UHPC-2%PP | 5° | 1.6 | 0.1 | 0.9 | 0.1 | 0.1 | 0.0 | 89 |
| | 20° | 17.7 | 8.4 | 12.5 | 6.2 | 1.5 | 0.5 | 50 |
| | 30° | 34.7 | 21.0 | 26.6 | 19.0 | 4.9 | 3.4 | 28 |

Note: *Mid-height recovery is the ratio of the elastic displacement (= peak displacement - residual displacement) and the peak displacement.

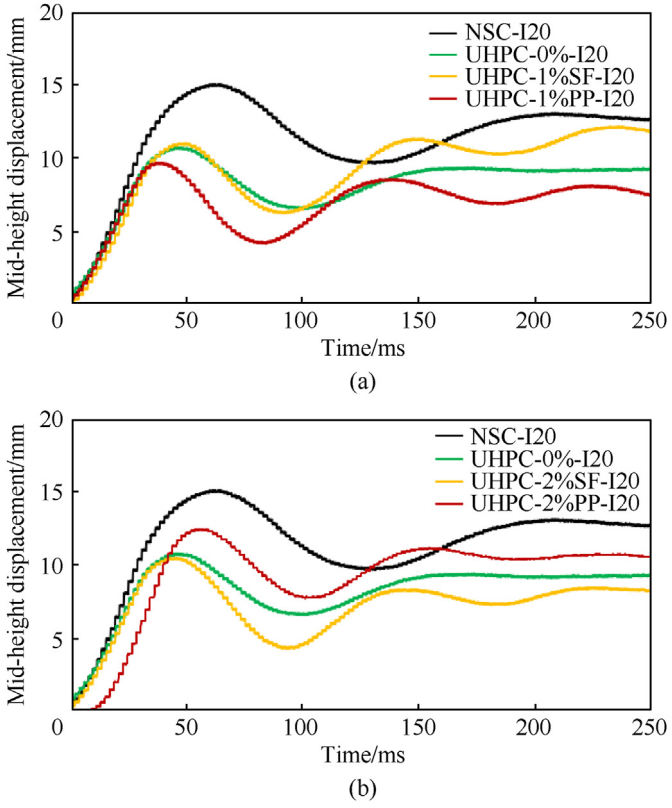


**Fig. 11.** Mid-height deflection-time histories (20° release angle): (a) Columns with 1% fibres vs reference columns; (b) Columns with 2% fibres vs reference columns.

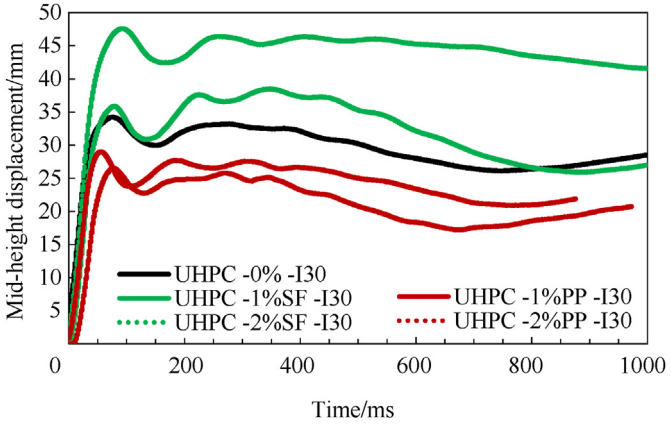


**Fig. 12.** Mid-height deflection-time histories (30° release angle).

NSC while the plastic displacement exhibits the column's capability to absorb energy. Interestingly, despite comparable mid-height displacement time histories, the comparison of deflection recovery between UHPC columns under 20° impact indicates that a steel fibre content of 1% produced the most elastic impact response.

The use of different fibre volume fractions (1% vs 2%) did not show a clear influence on the displacement, e.g., the maximum mid-height displacement of UHPC-1%SF was higher than that of UHPC-2%SF (12.2 mm vs 10.5 mm). However, Column UHPC-1%PP exhibited higher max mid-height displacement of 9.7 mm which was significantly lower than that of Column UHPC-2%PP.

The influence of the fibre type on the displacement of the columns was also very complicated. For 1% fibre volume fraction, the max mid-height displacement of Column UHPC-1%PP was significantly lower than that of UHPC-1%SF (9.7 mm vs 12.2 mm). However, the mid-height displacement of Column UHPC-2%PP (12.5 mm) was higher than that of Column UHPC-2%SF.

Therefore, it is difficult to draw a conclusive statement about the influence of either fibre type and fibre volume fraction on the displacement of these columns. In general, the use of fibre-reinforced UHPC significantly reduce the max mid-height displacement and the influence of PP micro-fibre was comparable to that of SF under 20° impact.

### 3.3.2. *Under 30° impact (2.58 m/s)*

Under 30° impact, all the columns exhibited greater max and residual displacement as shown in Fig. 12. Compared to Column UHPC-0%, the influence of fibre type (steel fibres vs PP micro-fibres) on the displacement was obvious, i.e., UHPC reinforced with steel fibres experienced higher maximum and residual displacement; On the other hand, UHPC with PP micro-fibres exhibited an obvious reduction in both maximum and residual displacement.

The use of steel fibres in UHPC increased the compressive strength, leading to higher contact and global stiffness. Therefore,

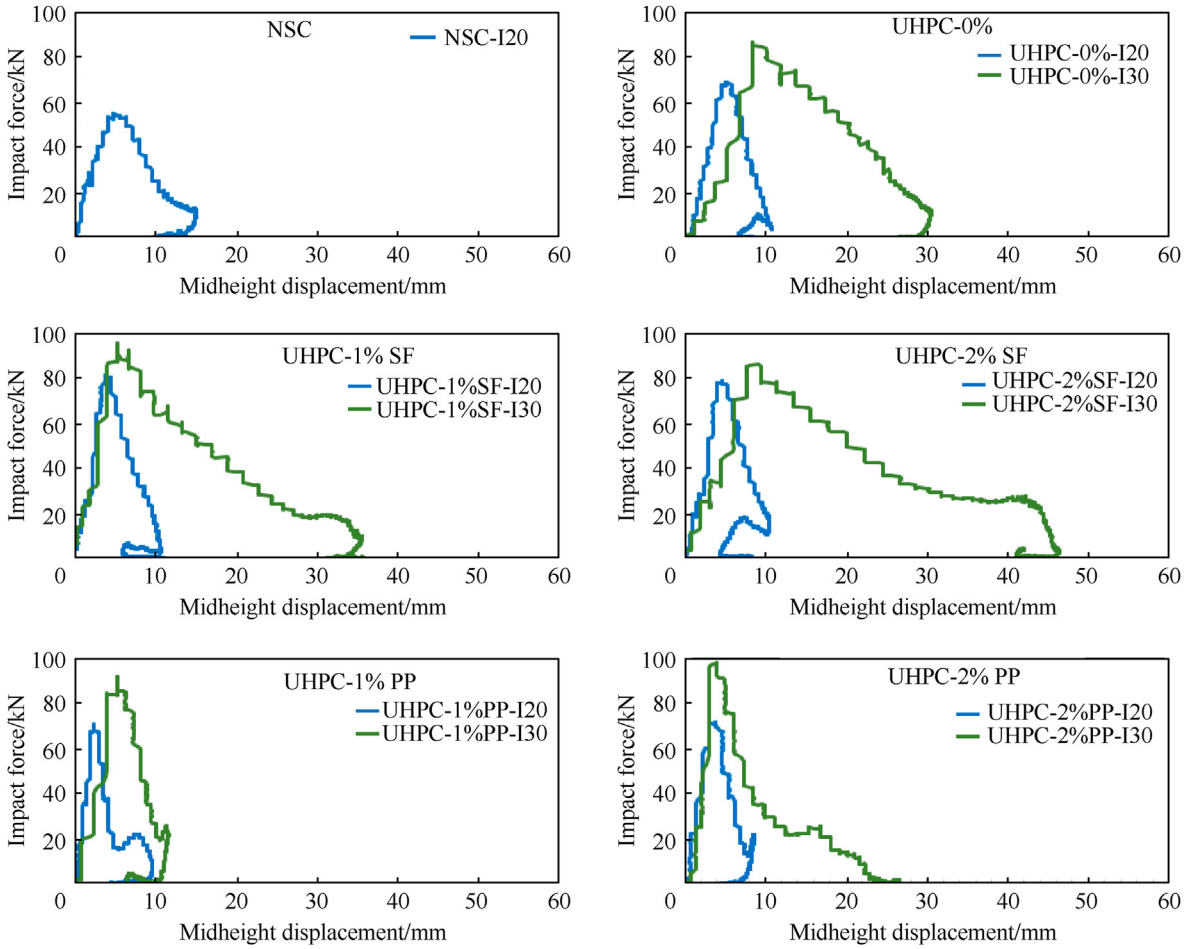


**Fig. 13.** Impact force-mid-height deflection graphs of all the columns.

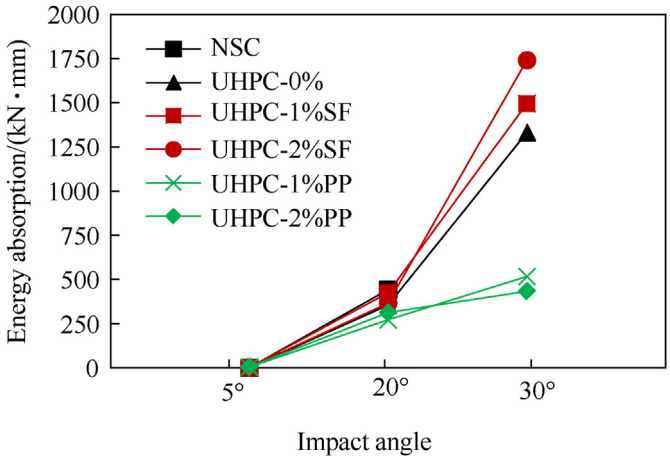


**Fig. 14.** Comparison of energy absorption by each column at different impact velocities.

the columns with steel fibres attracted higher impact force as shown in Fig. 7 and Table 5. The higher impact force resulted in larger displacement of these columns since the increase in the modulus could not counteract the influence of higher impact force.

On the other hand, UHPC reinforced with PP micro-fibres showed a marginal reduction in compressive strength but an increase in tensile strength as compared to UHPC-0% (see Table 5). The reduced compressive strength resulted in lower contact stiffness while the higher tensile strength improved the localised shear stiffness and resistance. These two factors affect the local stiffness in different ways. The experimental results showed that the maximum impact forces of the columns with PP micro-fibres were higher than Column UHPC-0% in all impact conditions. However, the max mid-height displacement of Columns UHPC-1%PP and UHPC-2%PP under 30° impact was 29 mm and 26.6 mm while the corresponding displacement of UHPC-0% was 34.3 mm, indicating a significant reduction. This observation was observed in the previous studies [32,33] which found that PP micro-fibre-reinforced concrete structures exhibited lower maximum and residual displacement under large deformation. The result of this study again confirms this observation.

**Table 7**
Energy absorption.

| Column | Energy absorption/(kN·mm) | |
|---|---|---|
| | Impact 20° | Impact 30° |
| NSC | 442 | – |
| UHPC-0% | 354 | 1332 |
| UHPC-1%SF | 424 | 1496 |
| UHPC-2%SF | 366 | 1742 |
| UHPC-1%PP | 271 | 517 |
| UHPC-2%PP | 312 | 434 |

It is noted that Column NSC exhibited large cracks, substantial residual displacement, and completely collapsed under 30° impact. It could be considered that Column NSC reached at 20° impact. Column UHPC-2%SF showed shear failure at the column base where the casting defect occurred. The shear failure might happen at the impact point but not the base if the column were cast perfectly. This failure was attributed to this weak section due to casting defect and therefore the results of displacement of these two columns are not discussed in this section.

In general, the use of fibres in UHPC not only significantly reduced both max and residual displacement but also substantially improved displacement recovery. The displacement performance of PP-reinforced UHPC was comparable and some cases better than that of SF-reinforced UHPC under impact loads.

### 3.4. Energy absorption

The toughness of UHPC is a combination of strength and ductility and measuring the toughness of UHPC often varies between studies [19]. In general, the toughness of structures is estimated based on the work done by the applied load, which is the area under the load-displacement curve [26,73]. However, under dynamic loading, where inertia resistance plays an important role, this method may not be appropriate when ignoring this effect. Under a hard impact, the two objects separate very quickly, for example steel projectile collides directly with concrete beam, using the enclosed area of the load-displacement to represent the energy absorption is not appropriate [33,74]. Some other studies used reaction force-displacement curve to estimate the energy absorption. This method also cannot consider the inertial effect and more discussions were presented in Ref. [33]. In the hard contact problem, the impactor was separated from concrete structures in about 1–5 ms while this study used a soft contact condition, at which the column and impactor were in contact for about 50 ms. This impact duration was long enough to adopt the conventional method using the enclosed impact force-displacement to quantify the energy absorption of the tested columns because the influence of the inertia force becomes less significant [33]. The impact force vs mid-height displacement and energy absorption of all the columns under all impacts are presented in Figs. 13 and 14 and Table 7.

In general, the use of UHPC with steel fibres improved the energy absorption of these columns. When the impact velocity was small (impact at 5° with a velocity of 0.44 mm), only elastic deformation was expected, as evidenced by zero energy absorption. When the impact velocity increased to 1.73 m/s, all these columns exhibited relatively similar energy absorption, indicating a very marginal influence of fibre reinforcement. The reference UHPC-0% column showed slightly higher energy absorption due to more damage. When subjected to a higher impact velocity (2.58 m/s), the influence of fibre volume fraction and fibre type became obvious as shown in Fig. 14. The energy absorption of Column NSC cannot be derived due to loss of displacement data. The use of steel fibres improved the energy absorption compared to that of Columns UHPC-0%. Columns UHPC-1%PP and UHPC-2%PP showed lower displacement than that of Columns UHPC-1%SF and UHPC-2%SF, thus, the first ones absorbed significantly less energy than the later ones. This phenomenon was attributed to less damage to the columns reinforced with PP micro-fibres and highly elastic behaviour of these fibres.

## 4. Conclusions

This study examined the impact behaviour of FRUHPC columns and investigated the effect of fibre volume fraction and type on their performance. Particular attention was paid on the use of PP fibre to improve the structural performance of PP reinforced UHPC columns while previous studies primarily used PP fibre for preventing shrinkage cracks or mitigating explosive spalling in concrete structures exposed to fire or subjected to impact/blast loads. The findings can be summarised as follows:

1) Macro steel fibres slightly reduced the workability of UHPC while marginally increased its compressive strength. Micro PP micro-fibres simultaneously declined the workability and compressive strength of UHPC.
2) Fibre reinforcement significantly improved the impact behaviour of FRUHPC columns, shifting the failure mechanism from brittle shear to flexural failure. All the columns failed by the combination of local and global modes under 30° impact (2.58 m/s).
3) The addition of fibre in UHPC only slightly changed the local stiffness of the columns, and its effect was based on the type of fibres. Steel fibre-reinforced UHPC considerably increased the peak impact force (up to 18%), while the use of PP micro-fibres only slightly increased the peak impact force (3%–4%).
4) The use of FRUHPC did not affect the impact duration of about 45–50 ms.
5) Fibre-reinforced UHPC significantly reduced the maximum mid-height displacement (up to 30% under 20° impact) and substantially improved the displacement recovery (up to 100% under 20° impact). The optimal fibre content for PP micro-fibres was found to be 1% due to low displacement and damage.
6) The columns reinforced with steel fibres showed great energy absorption while those with PP micro-fibres experienced a reduction in energy absorption.

Overall, the inclusion of fibres in UHPC overcomes the issue of brittle failure of traditional NSC columns under impact loading by creating a more favourable flexural failure mechanism as well as enhancing ductility and/or toughness. The following matters should be considered for better use of PP fibres in future studies:

1) Investigate the optimal fibre content: our study found that the optimal fibre content for PP micro-fibres was approximately at 1% due to low displacement and damage. Future studies could further investigate this finding, exploring a wider range of fibre content to optimize the performance of PP reinforced UHPC columns.
2) Study the impact of fibre reinforcement on other properties: this study found that fibre reinforcement significantly improved the impact behaviour of FRUHPC columns. Future research could explore the impact of fibre reinforcement on other properties of UHPC, such as tensile strength, flexural strength, and modulus of elasticity.
3) Address the bonding issues: current PP fibres do not have good bonding with concrete matrix. Future studies should focus on improving the bonding with matrix through surface modification, such as Shi et al. [75] who improve the bonding of PP fibre up to 121%.

## Declaration of competing interest

The authors declare no conflict of interests.

## Acknowledgement

The authors acknowledge the financial support from Australian Research Council (ARC) (Grant No. DP220100307).

## References


[1] Abdelkarim OI, ElGawady MA. Performance of bridge piers under vehicle collision. Eng Struct 2017;140(Supplement C):337–52.
[2] Wei J, Li J, Wu C. An experimental and numerical study of reinforced conventional concrete and ultra-high performance concrete columns under lateral impact loads. Eng Struct 2019;201:109822.
[3] Wu H, Hu F, Fang Q. A comparative study for the impact performance of shaped charge JET on UHPC targets. Defence Technology 2019;15(4):506–18.
[4] Murali G. Recent research in mechanical properties of geopolymer-based ultra-high-performance concrete: a review. Defence Technology 2024;32:67–88.
[5] Do TV, Pham TM, Hao H. Dynamic responses and failure modes of bridge columns under vehicle collision. Eng Struct 2018;156:243–59.
[6] Do TV, Pham TM, Hao H. Impact force profile and failure classification of reinforced concrete bridge columns against vehicle impact. Eng Struct 2019;183:443–58.
[7] Su Y, Li J, Wu C, Wu P, Li Z-X. Effects of steel fibres on dynamic strength of UHPC. Construct Build Mater 2016;114:708–18.
[8] Xia Y, Wu C, Liu Z-X, Yuan Y. Protective effect of graded density aluminium foam on RC slab under blast loading – an experimental study. Construct Build Mater 2016;111:209–22.
[9] Wei J, Li J, Wu C. Study on hybrid fibre reinforced UHPC beams under single and repeated lateral impact loading. Construct Build Mater 2023;368:130403.
[10] Xu S, Liu Z, Li J, Yang Y, Wu C. Dynamic behaviors of reinforced NSC and UHPC columns protected by aluminum foam layer against low-velocity impact. J Build Eng 2020:101910.
[11] Li J, Wu C, Hao H. Investigation of ultra-high performance concrete slab and normal strength concrete slab under contact explosion. Eng Struct 2015;102:395–408.
[12] Li J, Wu C, Hao H, Wang Z, Su Y. Experimental investigation of ultra-high performance concrete slabs under contact explosions. Int J Impact Eng 2016;93:62–75.
[13] Pournasiri E, Pham TM, Hao H. Structural performance evaluation of UHPC/conventional concrete cast on novel FRP stay-in-place formwork for concrete bridge decks. Structures 2022;41:1077–91.
[14] Pournasiri E, Pham TM, Hao H. Behaviour of ultra-high performance concrete (UHPC) bridge decks with new Y-shape FRP stay-in-place formworks. J Compos Construct 2022;26(3):04022023.
[15] Xiao Q-q, Huang Z-x, Zu X, Jia X, Zhu Q-f, Cai W. Shaped charge penetration into high- and ultrahigh-strength Steel–Fiber reactive powder concrete targets. Defence Technology 2020;16(1):217–24.
[16] Xue J, Briseghella B, Huang F, Nuti C, Tabatabai H, Chen B. Review of ultra-high performance concrete and its application in bridge engineering. Construct Build Mater 2020;260:119844.
[17] Shi C, Wu Z, Xiao J, Wang D, Huang Z, Fang Z. A review on ultra high performance concrete: Part I. Raw materials and mixture design. Construct Build Mater 2015;101:741–51.
[18] Portland Cement Association. Ultra-high performance concrete. 2023. https://www.cement.org/learn/concrete-technology/concrete-design-production/ultra-high-performance-concrete#:~:text=Ultra%2DHigh%20Performance%20Concrete%20(UHPC,mixture%20to%20achieve%20specified%20requirements. 18/04/2023.
[19] Wang D, Shi C, Wu Z, Xiao J, Huang Z, Fang Z. A review on ultra high performance concrete: Part II. Hydration, microstructure and properties. Construct Build Mater 2015;96:368–77.
[20] Abbas S, Nehdi M, Saleem M. Ultra-high performance concrete: mechanical performance, durability, sustainability and implementation challenges. International Journal of Concrete Structures and Materials 2016;10(3):271–95.
[21] Yan J, Zhang Q, Liu Y, Xu Y, Shi Z, Bai F, Huang F. Experimental and numerical analyses of the effect of fibre content on the close-in blast performance of a UHPFRC beam. Defence Technology 2024;31:242–61.
[22] Xu S, Liu Z, Li J, Yang Y, Wu C. Dynamic behaviors of reinforced NSC and UHPC columns protected by aluminum foam layer against low-velocity impact. J Build Eng 2021;34:101910.
[23] Su Y, Li J, Wu C, Wu P, Li Z-X. Influences of nano-particles on dynamic strength of ultra-high performance concrete. Composer Part B 2016;91:595–609.
[24] Wei J, Li J, Wu C. Behaviour of hollow-core and steel wire mesh reinforced ultra-high performance concrete columns under lateral impact loading. Int J Impact Eng 2020;146:103726.
[25] Chen Y, Matalkah F, Weerasiri R, Balachandra A, Soroushian P. Dispersion of fibers in ultra-high-performance concrete. Concr Int 2017;39(12):45–50.
[26] Shi F, Pham TM, Hao H, Hao Y. Post-cracking behaviour of basalt and macro polypropylene hybrid fibre reinforced concrete with different compressive strengths. Construct Build Mater 2020;262:120108.
[27] Sciarretta F, Fava S, Francini M, Ponticelli L, Caciolai M, Briseghella B, Nuti C. Ultra-High performance concrete (UHPC) with polypropylene (Pp) and steel Fibres: investigation on the high temperature behaviour. Construct Build Mater 2021;304:124608.
[28] Zhang D, Dasari A, Tan KH. On the mechanism of prevention of explosive spalling in ultra-high performance concrete with polymer fibers. Cement Concr Res 2018;113:169–77.
[29] Li Y, Pimienta P, Pinoteau N, Tan KH. Effect of aggregate size and inclusion of polypropylene and steel fibers on explosive spalling and pore pressure in ultra-high-performance concrete (UHPC) at elevated temperature. Cem Concr Compos 2019;99:62–71.
[30] Zhang D, Zhang Y, Dasari A, Tan KH, Weng Y. Effect of spatial distribution of polymer fibers on preventing spalling of UHPC at high temperatures. Cement Concr Res 2021;140:106281.
[31] Xiong M-X, Liew JR. Spalling behavior and residual resistance of fibre reinforced Ultra-High performance concrete after exposure to high temperatures. Mater Construcción 2015;65(320):e071. e071.
[32] Ngo TT, Pham TM, Hao H, Chen W, Elchalakani M. Performance of monolithic and dry joints with GFRP bolts reinforced with different fibres and GFRP bars under impact loading. Eng Struct 2021;240:112341.
[33] Tran TT, Pham TM, Huang Z, Chen W, Hao H, Elchalakani M. Effect of fibre reinforcements on shear capacity of geopolymer concrete beams subjected to impact loads. Int J Impact Eng 2022;159:104056.
[34] Latifi MR, Biricik Ö, Mardani Aghabaglou A. Effect of the addition of polypropylene fiber on concrete properties. J Adhes Sci Technol 2022;36(4):345–69.
[35] A. 3972. General purpose and blended cements, AS 3972. Sydney, Australia: Standards Australia; 2010.
[36] SIMCOA Silica Fume. Silicon metal company of Australia. SIMCOA; 2021.
[37] Tran TT, Pham TM, Hao H. Experimental and analytical investigation on flexural behaviour of ambient cured geopolymer concrete beams reinforced with steel fibers. Eng Struct 2019;200:109707.
[38] T.A.P. Ltd, TEXO. 2016. http://texo.net.au/steel-fibre. http://texo.net.au/. Jan 31, 2019.
[39] Nguyen DL, Ryu GS, Koh KT, Kim DJ. Size and geometry dependent tensile behavior of ultra-high-performance fiber-reinforced concrete. Composer Part B 2014;58:279–92.
[40] Yoo D-Y, Kim S, Park G-J, Park J-J, Kim S-W. Effects of fiber shape, aspect ratio, and volume fraction on flexural behavior of ultra-high-performance fiber-reinforced cement composites. Compos Struct 2017;174:375–88.
[41] Wu Z, Khayat KH, Shi C. How do fiber shape and matrix composition affect fiber pullout behavior and flexural properties of UHPC? Cem Concr Compos 2018;90:193–201.
[42] Song Q, Yu R, Shui Z, Wang X, Rao S, Lin Z, Wang Z. Key parameters in optimizing fibres orientation and distribution for ultra-high performance fibre reinforced concrete (UHPFRC). Construct Build Mater 2018;188:17–27.
[43] Balanji EKZ, Sheikh MN, Hadi MNS. Behaviour of high strength concrete reinforced with different types of steel fibres. Aust J Struct Eng 2017;18(4):254–61.
[44] Tran TT, Pham TM, Hao H. Effect of hybrid fibers on shear behaviour of geopolymer concrete beams reinforced by basalt fiber reinforced polymer (BFRP) bars without stirrups. Compos Struct 2020;243:112236.
[45] Tran DT, Pham TM, Hao H, Ha NS, Vo NH, Chen W. Precast segmental beams made of fibre-reinforced geopolymer concrete and FRP tendons and reinforcement against impact loads. Eng Struct 2023;295:116862.
[46] Dang TD, Tran DT, Nguyen-Minh L, Nassif AY. Shear resistant capacity of steel fibres reinforced concrete deep beams: an experimental investigation and a new prediction model. Structures 2021;33:2284–300.
[47] Liu J, Wu C, Su Y, Li J, Shao R, Chen G, Liu Z. Experimental and numerical studies of ultra-high performance concrete targets against high-velocity projectile impacts. Eng Struct 2018;173:166–79.
[48] Liu J, Wu C, Li J, Su Y, Shao R, Liu Z, Chen G. Experimental and numerical study of reactive powder concrete reinforced with steel wire mesh against projectile penetration. Int J Impact Eng 2017;109:131–49.
[49] Pham TM, Zhang X, Elchalakani M, Karrech A, Hao H, Ryan A. Dynamic response of rubberized concrete columns with and without FRP confinement subjected to lateral impact. Construct Build Mater 2018;186:207–18.
[50] Schoettler MJ, Restrepo JI, Guerrini G, Duck DE, Carrea F. A full-scale, single-column bridge bent tested by shake-table excitation, center for civil engineering earthquake research, department of civil engineering. University of Nevada; 2012.
[51] AS 5100.2:2017. Bridge design, Part 2: design loads. 2017. Sydney, NSW, Australia.
[52] Li C, Bi K, Hao H. Seismic performances of precast segmental column under bidirectional earthquake motions: shake table test and numerical evaluation. Eng Struct 2019;187:314–28.
[53] AS 1012.2. Methods of testing concrete; method 2: preparation of the concrete mixes in the laboratory. 2014.
[54] AS 1012.3.1, Determination of properties related to consistency of concrete-Slump test. Sydney: Standards Australia; 2014.
[55] AS 1012.9. Compressive strength tests - concrete, 1012.9: 2014. 2014. Sydney, NSW, Australia.
[56] AS 1012.10. Methods of testing concrete Determination of indirect tensile strength of concrete cylinders ('Brazil' or splitting test) (Reconfirmed 2014). 2000. 1012.10: 2000, Sydney, NSW, Australia.
[57] Ireland DR. In: DeSisto TS, editor. Procedures and problems associated with reliable control of the instrumented impact test. West Conshohocken, PA: ASTM International; 1974. p. 3–29.
[58] Suaris W, Shah SP. Inertial effects in the instrumented impact testing of cementitious composites. Cem Concr Aggregates 1981;3(2):77–83.
[59] Tran TT, Pham TM, Huang Z, Chen W, Ngo TT, Hao H, Elchalakani M. Effect of fibre reinforcements on shear capacity of geopolymer concrete beams subjected to impact load. Int J Impact Eng 2022;159:104056.
[60] Li H, Chen W, Huang Z, Hao H, Ngo TT, Pham TM. Influence of various impact

scenarios on the dynamic performance of concrete beam-column joints. Int J Impact Eng 2022;167:104284.
[61] Cotsovos DM, Stathopoulos ND, Zeris CA. Behavior of RC beams subjected to high rates of concentrated loading. J Struct Eng 2008;134(12):1839–51.
[62] Fujikake K, Li B, Soeun S. Impact response of reinforced concrete beam and its analytical evaluation. J Struct Eng 2009;135(8):938–50.
[63] Pham TM, Hao H. Behavior of fiber-reinforced polymer-strengthened reinforced concrete beams under static and impact loads. Int J Prot Struct 2016;8(1):3–24.
[64] Pham TM, Hao H. Plastic hinges and inertia forces in RC beams under impact loads. Int J Impact Eng 2017;103:1–11.
[65] Pham TM, Hao Y, Hao H. Sensitivity of impact behaviour of RC beams to contact stiffness. Int J Impact Eng 2018;112:155–64.
[66] Huang Z, Chen W, Hao H, Chen Z, Pham TM, Tran TT, Elchalakani M. Shear behaviour of ambient cured geopolymer concrete beams reinforced with BFRP bars under static and impact loads. Eng Struct 2021;231:111730.
[67] Tran TT, Pham TM, Huang Z, Chen W, Hao H, Elchalakani M. Impact response of fibre reinforced geopolymer concrete beams with BFRP bars and stirrups. Eng Struct 2021;231:111785.
[68] Pham TM, Chen W, Elchalakani M, Do TV, Hao H. Sensitivity of lateral impact response of RC columns reinforced with GFRP bars and stirrups to concrete strength and reinforcement ratio. Eng Struct 2021;242:112512.
[69] Pham TM, Hao H. Effect of the plastic hinge and boundary condition on the impact behaviour of RC beams. Int J Impact Eng 2017;102:74–85.
[70] Pham TM, Hao H. Influence of global stiffness and equivalent model on prediction of impact response of RC beams. Int J Impact Eng 2018;113:88–97.
[71] Li H, Chen W, Pham TM, Hao H. Analytical and numerical studies on impact force profile of RC beam under drop weight impact. Int J Impact Eng 2021;147:103743.
[72] Riedel P, Leutbecher T, Piotrowski S, Heese C. Einfluss der Probekörpergeometrie auf die Ergebnisse von Druckfestigkeitsprüfungen an ultrahochfestem Beton. Beton-und Stahlbetonbau 2018;113(8):598–607.
[73] ASTM C1018. Standard test method for flexural toughness and first-crack strength of fiber-reinforced concrete (using beam with third-point loading), ASTM C1018:97. West Conshohocken, PA: ASTM International; 1997.
[74] Pham TM, Chen W, Elchalakani M, Karrech A, Hao H. Experimental investigation on lightweight rubberized concrete beams strengthened with BFRP sheets subjected to impact loads. Eng Struct 2020;205:110095.
[75] Shi F, Yin S, Pham TM, Tuladhar R, Hao H. Pullout and flexural performance of silane groups and hydrophilic groups grafted polypropylene fibre reinforced UHPC. Construct Build Mater 2021;277:122335.